

Plasmon-Enhanced Ultraviolet Photoluminescence from Hybrid Structures of Graphene/ZnO Films

Sung Won Hwang,¹ Dong Hee Shin,¹ Chang Oh Kim,¹ Seung Hui Hong,¹ Min Choul Kim,¹ Jungkil Kim,¹ Keun Yong Lim,¹ Sung Kim,¹ Suk-Ho Choi,^{1,*} Kwang Jun Ahn,² Gunn Kim,³ Sung Hyun Sim,⁴ and Byung Hee Hong⁴

¹*Department of Applied Physics, College of Applied Science, Kyung Hee University, Yongin 446-701, Korea*

²*School of Physics and Astronomy, Seoul National University, Seoul 151-747, Korea*

³*Department of Physics, Kyung Hee University, Seoul 130-701, Korea*

⁴*Department of Chemistry, SKKU Advanced Institute of Nanotechnology, Sungkyunkwan University, Suwon 440-746, Korea*

(Received 6 January 2010; published 15 September 2010)

We report substantially enhanced photoluminescence (PL) from hybrid structures of graphene/ZnO films at a band gap energy of ZnO (~ 3.3 eV/376 nm). Despite the well-known constant optical conductivity of graphene in the visible-frequency regime, its abnormally strong absorption in the violet-frequency region has recently been reported. In this Letter, we demonstrate that the resonant excitation of graphene plasmon is responsible for such absorption and eventually contributes to enhanced photoemission from structures of graphene/ZnO films when the corrugation of the ZnO surface modulates photons emitted from ZnO to fulfill the dispersion relation of graphene plasmon. These arguments are strongly supported by PL enhancements depending on the spacer thickness, measurement temperature, and annealing temperature, and the micro-PL mapping images obtained from separate graphene layers on ZnO films.

DOI: 10.1103/PhysRevLett.105.127403

PACS numbers: 78.66.Jg, 73.21.-b, 78.55.Et, 78.66.Qn

Graphene is a single atomic layer of graphite [1]. Since the successful isolation of graphene from graphite and transfer onto dielectric substrates, significant efforts have been devoted to determine the electrical and optical properties of graphene [2–4]. Carriers in graphene show Dirac-fermionic energy dispersion linearly depending on the excitation momentum with high Fermi velocity and zero band gap due to the crystal symmetry of graphene, wherein the carbon atoms are covalently bonded in two-dimensional hexagonal form [1,5]. It is currently possible to engineer the band gap and the Fermi energy of graphene through electrical gating and carrier doping [6,7].

In addition to mobility, high optical transparency is another characteristic feature of graphene. It has been theoretically [8] and experimentally [9,10] shown that the quasiuniform transmittance of graphene maintained up to the visible range originates from the optical conductivity provided by a constant value of $e^2/4\hbar$, where e is the elementary charge and \hbar Planck's constant divided by 2π .

Alternatively, there are several reports of abnormally increased absorption of graphene in the violet-frequency region [10,11]. R. R. Nair, *et al.* [10] found that the unexpected absorption was attributed to the excitation of spectrally broadened surface plasmonic modes in graphene and the breakdown of the Dirac-fermion model, caused by triangular warping and nonlinearity of energy bands far from the Dirac energy. In contrast, other studies [8,11] have demonstrated that the latter could have negligible influence on the optical conductivity. Optical properties of graphene in the violet-frequency regime is especially important for both isolated graphene and graphene graphitized on SiC substrates as the nearest-neighbor hopping

energy (~ 2.8 eV) [1,12] and the band gap energy of SiC (~ 3 eV) [12] are included in this frequency band.

In this Letter, we report substantially enhanced photoluminescence (PL) from hybrid structures of graphene/ZnO films at the band gap energy of ZnO (~ 3.3 eV). By comparing PL signals from samples fabricated in controlled manners, we demonstrate that the enhanced PL can be explained by the resonant excitation of graphene plasmon followed by its transformation into propagating photons through the interaction with the corrugated ZnO surface.

Background.—ZnO films typically exhibit PL spectra in the visible and ultraviolet ranges. Surface plasmon (SP)-mediated PL enhancement has already been observed at metal or metal alloy/ZnO interfaces [13–15], where radiation from ZnO film excites localized SP. Metallic properties of single-walled carbon nanotubes (SWCNTs) are also responsible for the SP-coupled PL enhancement observed in hybrid structures of SWCNTs/ZnO films [16]. Similar PL enhancement can be expected when a semimetallic graphene is attached on a ZnO film as schematically illustrated in Fig. 1(a). Resonant plasmon modes can be induced in graphene when the radiation from the ZnO film is partially trapped between the graphene and a ZnO surface and modulated by surface corrugation defined as a in Fig. 1(b). The induced plasmon can then be transformed into propagating photons through the scattering with granules on the ZnO surface and eventually result in enhanced photoemission.

The resonance condition and relaxation time of plasmonic modes in graphene are estimated as two leading factors for enhanced PL. Despite the similar electromagnetic expression of plasmon in graphene [17] and SP in thin

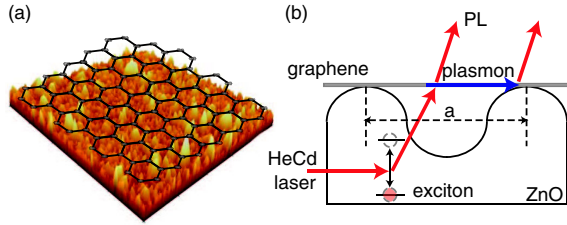


FIG. 1 (color online). (a) Illustration of a sample: graphene of a two-dimensional honeycomb structure on a SEM image of a ZnO film annealed at 900 °C. (b) Schematically depicted PL enhancement from a graphene/ZnO hybrid structure.

metal films [18], the most distinctive feature of graphene plasmon from SP is its high frequency limit with increasing momentum. While the SP frequency at an air-metal interface converges to $\omega_p/\sqrt{2}$, where ω_p is the plasma frequency of metal, graphene plasmon maintains its linear dispersion relation up to higher energies [12,19]. From several experimental [20–24] and theoretical studies [17,25–27] the in-plane wave number q -dependent energy dispersion relation of graphene plasmon $\omega(q)$ can be expressed in the random phase approximation [23,24] as

$$\omega(q) = \left[\frac{n_e e^2}{\epsilon_0(1 + \epsilon_b)m^*} q + \frac{3}{4} v_F^2 q^2 \right]^{1/2}, \quad (1)$$

where n_e is the number of electrons in a unit area, ϵ_0 is the vacuum permittivity, ϵ_b is the background dielectric constant, m^* is the effective mass of the graphene electrons, and v_F is the Fermi velocity. Here, we assume that graphene is surrounded by air ($\epsilon_b = 1$) because graphene is simply placed on the granular ZnO surface [28] without any chemical bonding and therefore in contact with air on both sides as in the case for SWCNTs [16,29]. With numerical parameters $n_e = 1 \times 10^{13} \text{ cm}^{-2}$ obtained by Hall measurements [3,30], $m^* = 0.077m_e$ [21], where m_e denotes electron mass, and $v_F = 1.12 \times 10^6 \text{ m/s}$ [21,23,26], the graphene plasmon can be resonantly excited at the band gap energy of ZnO ($\sim 3.3 \text{ eV}$) for an in-plane momentum $q = 2\pi/1.5 \text{ nm}^{-1}$. Therefore, if the surface corrugation of the ZnO film can be specified by the same modulus ($a \sim 1.5 \text{ nm}$), enhanced PL from the graphene/ZnO hybrid structure can be expected. At present, it is impossible to precisely measure the corrugation of the ZnO film because 1.5 nm is far below the resolution limit of the existing lateral-structure analysis techniques. However, it is believed that the corrugation of the ZnO surface is on the order of nm.

Furthermore, the relaxation time of graphene plasmon is considered. According to experimental [23,24] and theoretical [17] reports on plasmon damping in graphene, plasmon in the high frequency regime with a large momentum rapidly decays via electron-hole pair generation as well as the interaction with optical phonons. The relaxation time of the graphene plasmon is estimated as a few fs at the band gap energy of ZnO from its inversely quasilinear

behavior with frequency [23]. We should note that this time scale is determined without nonlocal screening by the substrate. The relaxation time can substantially increase when the Coulomb interaction within graphene is screened by the radiation from the ZnO substrate [12,17,23]. Moreover, the estimated relaxation time of graphene plasmon is comparable to that of SP in Ag/graphite hybrid systems ($\sim 10 \text{ fs}$) [31], where enhanced PL by SP has already been observed.

Experiments.—The samples were prepared as follows. 100 nm ZnO films were deposited on p -type Si (100) wafers at room temperature (RT) by RF magnetron sputtering and some of the films were annealed for 3 min under oxygen ambient to enhance their optical properties. Details of ZnO sputtering were described elsewhere [32]. Graphene layers were derived through mechanical exfoliation of highly oriented-pyrolithic-graphite (HOPG) and subsequently transferred to a 100-nm-thick ZnO film/ p -type Si wafers. The PL spectra were measured in a closed-cycle refrigerator by using a 325 nm line of HeCd laser as an excitation source. The microscopic (μ)-PL measurements were performed at RT using a home-built scanning confocal microscope. The laser beam was focused on the sample surface through a microscope objective that can focus the laser spot down to less than 1 μm . μ -PL signals from samples were spectrally dispersed by a 50 cm spectrometer equipped with a charge coupled device (Andor DU401A-BU). PL mapping was obtained by moving the sample under the microscope using properly aligned step motors. The spatial resolution of the PL mapping image was less than 2 μm . The graphene formed on the ZnO films was characterized by Raman spectroscopy, atomic-force microscopy (AFM), and optical microscopy. The experimental results and their analyses are in the supplementary information.

Figure 2(a) shows the PL spectra of a typical hybrid structure of graphene/ZnO film and a bare ZnO film at RT. The PL peak of the hybrid structure does not shift with respect to that of bare ZnO film ($\sim 376 \text{ nm}/3.30 \text{ eV}$), and the strongest PL peak intensity from the hybrid structure is approximately 4 times larger than that of bare ZnO film. The integrated PL intensity of the hybrid sample with respect to that of the bare ZnO film, the PL enhancement ratio, is plotted as a function of measurement temperature in Fig. 2(b). The enhancement ratio increases with decreasing temperature, similar to the PL behaviors in metal-capped ZnO films due to the coupling between the radiation field from ZnO and SP in metal [15].

The photoemissions from single-layer graphene (SG) and few-layer graphene (FG) on the ZnO film can not be distinguished by the conventional PL spectroscopy because the beam-spot size of the excitation source completely covered the graphene flakes. Therefore, the PL spectrum of the hybrid structure in Fig. 2(a) actually contains all PL signals from graphene with a different number

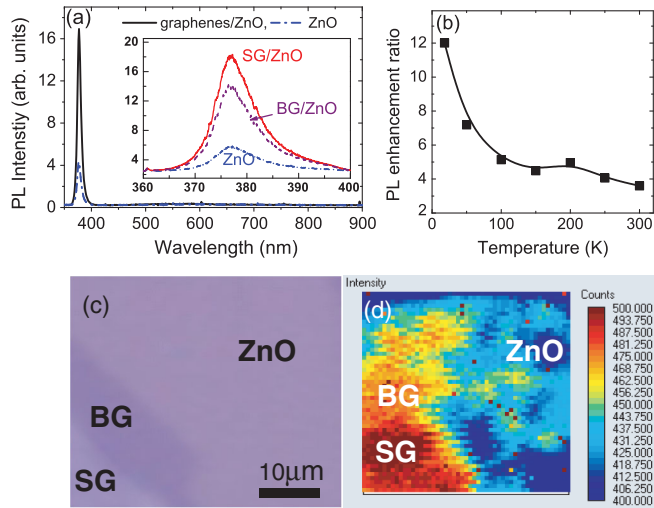


FIG. 2 (color). (a) PL spectra from a hybrid structure of graphene/ZnO film and a bare ZnO film. The inset shows PL spectra of single-layer (SG) and bilayer (BG) graphene/ZnO film and a bare ZnO film that were measured by micro-PL spectroscopy. (b) The dependence of PL enhancement ratio on the measurement temperature. (c) Optical microscopy image of a hybrid structure of graphene/ZnO film. The SG and BG regions are clearly distinct from the bare ZnO surface. (d) The corresponding micro-PL mapping image. The scales of the microscopy and PL mapping images are identical. The ZnO film was annealed at 900 °C.

of layers on the ZnO film. The inset of Fig. 2(a) shows PL spectra from separate SG, bilayer graphene (BG), and the bare surface on a ZnO film measured at RT by μ -PL spectroscopy. The μ -PL intensities are 3.2 and 2.4 times larger in SG and BG on the ZnO film, respectively, compared to that of the bare ZnO film. To confirm that the different PL enhancements are attributed to the number of graphene layers, two other samples with clearly distinguished, SG, BG, and bare surface regions on a ZnO film were fabricated.

For an example, an optical microscopic image and corresponding spatial mapping of μ -PL peak intensities are shown in Figs. 2(c) and 2(d), respectively. Peak intensities in the SG region are stronger than those in the BG region, which are larger than the intensities on the bare ZnO surface, consistent with the result of inset in Fig. 2(a). The smaller PL intensity of the BG region possibly results from a decrease in the optical transparency of the BG and a deviation from the plasmon-excitation condition of Eq. (1). As the number of graphene layers increases, the enhanced metallic feature due to the interlayer interaction of carriers [1] and the electron-phonon interaction [24] lead to a decrease in transmittance [10,33] and a different plasmon-dispersion behavior [24], respectively. The plasmon coupling is expected to increase at low temperatures due to the increase of plasmon density of states [15] and the reduction of plasmon damping caused by the electron-phonon

interaction [34], thereby increasing the PL enhancement ratio, as shown in Fig. 2(b).

The PL intensity of the hybrid structures strongly depends on the distance between the ZnO film and the graphene layer. Figure 3(a) shows an exponential decrease of the PL enhancement ratio as the thickness of the SiO₂ spacer between the ZnO film and graphene increases, resulting from the evanescent nature of graphene plasmon [17]. These results demonstrate that the enhanced PL from the hybrid structures of graphene/ZnO films originate from photons transformed from graphene plasmon via the scattering with corrugated ZnO surface.

All the PL data shown above were obtained using ZnO films annealed at 900 °C. Hybrid structures with ZnO films annealed at different temperatures were also prepared to study the influence of the film roughness on the PL enhancement. The right vertical axis in Fig. 3(b) shows the PL enhancement ratio as a function of annealing temperature (T_A). While reduction rather than enhancement in PL is observed up to $T_A = 600$ °C, the PL enhancement ratio sharply increases at $T_A = 900$ °C. It has been reported that the surface roughness of ZnO films increases after annealing at 900 °C [35,36]. Similar behavior of the surface roughness in ZnO films was observed with AFM, as presented in the left axis of Fig. 3(b), wherein the surface roughness profoundly increases at $T_A = 900$ °C. The scanning electron microscopy images show very different surface morphologies at $T_A = 900$ °C as well [37]. These results suggest that the surface conditions are crucial factors for the plasmon-assisted PL enhancement.

Similar experiments were performed with graphene produced by chemical vapor deposition (CVD) as detailed previously [4]. PL enhancement was not observed from the CVD samples by conventional PL spectroscopy or by μ -PL spectroscopy [37]. The conductivity of the CVD-grown graphene is estimated as 5 to 10 times less than that of the HOPG-derived graphene according to the previously reported values of their mobility and electron concentration [2–4,30,33,38]. This decrease is possibly due to the polycrystalline nature of the CVD-grown graphene which corroborates the reduction of PL in CVD-grown graphene/ZnO structures.

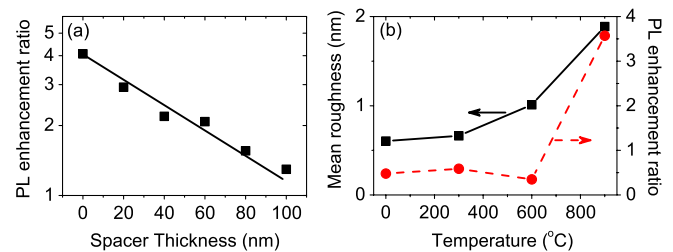


FIG. 3 (color online). (a) The PL enhancement ratio as a function of SiO₂-spacer thickness (b) Root-mean-square (rms) roughness of ZnO films (left vertical axis) and PL enhancement ratio (right vertical axis) as functions of annealing temperature.

In summary, substantially enhanced PL from hybrid structures of graphene/ZnO films at the band gap energy of ZnO compared to that from a bare ZnO film was experimentally observed. The enhanced PL was attributed to the resonant excitation of graphene plasmon and its transformation into propagating photons via the interaction with corrugated ZnO surface based on μ -PL mapping images obtained from separate graphene layers and PL data depending on the spacer thickness, measurement temperature, and annealing temperature. These results suggest that graphene is a promising candidate for potential application in highly efficient optoelectronic devices in visible and ultraviolet frequency regime.

*sukho@khu.ac.kr

- [1] A.H. Castro Neto, F. Guinea, N.M.R. Peres, K.S. Novoselov, and A.K. Geim, *Rev. Mod. Phys.* **81**, 109 (2009).
- [2] K.S. Novoselov, A.K. Geim, S.V. Morozov, D. Jiang, Y. Zhang, S.V. Dubonos, I.V. Grigorieva, and A.A. Firsov, *Science* **306**, 666 (2004).
- [3] K.S. Novoselov, A.K. Geim, S.V. Morozov, D. Jiang, M.I. Katsnelson, I.V. Grigorieva, S.V. Dubonos, and A.A. Firsov, *Nature (London)* **438**, 197 (2005).
- [4] K.S. Kim, Y. Zhao, H. Jang, S.Y. Lee, J.M. Kim, K.S. Kim, J.-H. Ahn, P. Kim, J.-Y. Choi, and B.H. Hong, *Nature (London)* **457**, 706 (2009).
- [5] A.K. Geim and K.S. Novoselov, *Nature Mater.* **6**, 183 (2007).
- [6] Y. Zhang, T.-T. Tang, C. Girit, Z. Hao, M.C. Martin, A. Zettl, M.F. Crommie, Y.R. Shen, and F. Wang, *Nature (London)* **459**, 820 (2009).
- [7] Feng Wang, Yuanbo Zhang, Chuanshan Tian, Caglar Girit, Alex Zettl, Michael Crommie, and Y. Ron Shen, *Science* **320**, 206 (2008).
- [8] T. Stauber, N.M.R. Peres, and A.K. Geim, *Phys. Rev. B* **78**, 085432 (2008).
- [9] Kin Fai Mak, Matthew Y. Sfeir, Yang Wu, Chun Hung Lui, James A. Misewich, and Tony F. Heinz, *Phys. Rev. Lett.* **101**, 196405 (2008).
- [10] R.R. Nair, P. Blake, A.N. Grigorenko, K.S. Novoselov, T.J. Booth, T. Stauber, N.M.R. Peres, and A.K. Geim, *Science* **320**, 1308 (2008).
- [11] Jahan M. Dawlaty, Shriram Shivaraman, Jared Strait, Paul George, Mvs Chandrashekhara, Farhan Rana, Michael G. Spencer, Dmitry Veksler, and Yunqing Chen, [arXiv:0801.3302v3](https://arxiv.org/abs/0801.3302v3).
- [12] Aaron Bostwick, Taisuke Ohta, Thomas Seyller, Karsten Horn, and Eli Rotenberg, *Nature Phys.* **3**, 36 (2007).
- [13] D.Y. Lei, J. Li, and H.C. Ong, *Appl. Phys. Lett.* **91**, 021112 (2007).
- [14] W.H. Ni, J. An, C.W. Lai, H.C. Ong, and J.B. Xu, *J. Appl. Phys.* **100**, 026103 (2006).
- [15] J. Li and H.C. Ong, *Appl. Phys. Lett.* **92**, 121107 (2008).
- [16] S. Kim, D.H. Shin, C.O. Kim, S.W. Hwang, S.-H. Choi, S. Ji, and J.-Y. Koo, *Appl. Phys. Lett.* **94**, 213113 (2009).
- [17] Marinko Jablan, Hrvoje Buljan, and Marin Soljačić, *Phys. Rev. B* **80**, 245435 (2009).
- [18] H. Raether, *Surface Plasmons on Smooth and Rough Surfaces and on Gratings*, Springer Tracts in Modern Physics (Springer-Verlag, Berlin, 1988), Vol. 111.
- [19] Chel-Hwang Park, Feliciano Giustino, Marvin L. Cohen, and Steven G. Louie, *Phys. Rev. Lett.* **99**, 086804 (2007).
- [20] Mhairi H. Gass, Ursel Bangert, Andrew L. Bleloch, Peng Wang, Rahul. R. Nair, and A.K. Geim, *Nature Nanotech.* **3**, 676 (2008).
- [21] T. Eberlein, U. Bangert, R.R. Nair, R. Jones, M. Gass, A.L. Bleloch, K.S. Novoselov, A. Geim, and P.R. Briddon, *Phys. Rev. B* **77**, 233406 (2008).
- [22] C. Kramberger, R. Hambach, C. Giorgetti, M.H. Rummeli, M. Knupfer, J. Fink, B. Büchner, L. Reining, E. Einarsson, S. Maruyama, F. Sottile, K. Hannewald, V. Olevano, A.G. Marinopoulos, and T. Pichler, *Phys. Rev. Lett.* **100**, 196803 (2008).
- [23] Yu Liu, R.F. Willis, K.V. Emtsev, and Th. Seyller, *Phys. Rev. B* **78**, 201403(R) (2008).
- [24] Yu Liu and R.F. Willis, *Phys. Rev. B* **81**, 081406(R) (2010).
- [25] E.H. Hwang and S. Das Sarma, *Phys. Rev. B* **75**, 205418 (2007).
- [26] P.E. Trevisanutto, C. Giorgetti, L. Reining, M. Ladisa, and V. Olevano, *Phys. Rev. Lett.* **101**, 226405 (2008).
- [27] S. Das Sarma and E.H. Hwang, *Phys. Rev. Lett.* **102**, 206412 (2009).
- [28] H.R. Kim, S. Kim, C.O. Kim, and S.-H. Choi, *Thin Solid Films* **518**, 305 (2009).
- [29] Q. Lu, R. Rao, B. Sadanadan, W. Que, A.M. Rao, and P.C. Ke, *Appl. Phys. Lett.* **87**, 173102 (2005).
- [30] Y. Zhang, Y.-W. Tan, H.L. Stormer, and P. Kim, *Nature (London)* **438**, 201 (2005).
- [31] J. Lehmann, M. Mershdorf, W. Pfeiffer, A. Thon, S. Voll, and G. Gerber, *Phys. Rev. Lett.* **85**, 2921 (2000).
- [32] D.K. Lee, S. Kim, M.C. Kim, S.H. Eom, H.T. Oh, and S.-H. Choi, *J. Korean Phys. Soc.* **51**, 1378 (2007).
- [33] X. Li, W. Cai, J. An, S. Kim, J. Nah, D. Yang, R. Piner, A. Velamakanni, I. Jung, E. Tutuc, S.K. Banerjee, L. Colombo, and R.S. Ruoff, *Science* **324**, 1312 (2009).
- [34] M. Liu, M. Pelton, and P. Guyot-Sionnest, *Phys. Rev. B* **79**, 035418 (2009).
- [35] J. Y. Lee, H. S. Kim, J. H. Chang, M. Yang, H. S. Ahn, and S. O. Ryu, *Jpn. J. Appl. Phys.* **44**, L205 (2005).
- [36] Y.G. Wang, S.P. Lau, X.H. Zhang, H.H. Hng, H.W. Lee, S.F. Yu, and B.K. Tay, *J. Cryst. Growth* **259**, 335 (2003).
- [37] See supplementary material at <http://link.aps.org/supplemental/10.1103/PhysRevLett.105.127403>.
- [38] D. Wei, Y. Liu, Y. Wang, H. Zhang, L. Huang, and G. Yu, *Nano Lett.* **9**, 1752 (2009).